Reflective Filtered Backprojection

Jean-Baptiste Bellet, Gérard Berginc

REFLECTIVE FILTERED BACKPROJECTION

JEAN-BAPTISTE BELLET AND GÉRARD BERGINC

Abstract. We propose a study about the filtered backprojection on reflective-kind projections. A reflective projection is defined, tomographic filtering of such a projection is analysed, and so is the filtered backprojection. The results emphasize the role of the contrasts of the projections and show what the contribution of the original scene is.

1. Introduction

The Radon transform encounters a great success in transmission tomography by X-Ray: since transmission models involve the Radon transform, numerical reconstruction of media are provided by inversion of the Radon transform [9]. The filtered backprojection (FBP) methods are among the most famous inversion algorithms. The use of FBP has been extended to other kind of imaging modalities by several authors [4, 8, 10]. In particular, altough one of the main components of laser images comes from backscattering by opaque surfaces, which differs from transmission, the FDK algorithm is at the heart of a 3D laser imaging technique which is emerging [1–6]. The success of this laser FDK algorithm suggests that FBP works also in reflection imaging, and does not require a complete view (scan over 360 degrees) to provide interesting reconstructions using such data. Nevertheless, according to the authors' knowledge, FBP on reflection data has never been studied in a mathematical framework. This is the object of this Note: we give a meaning to this reflective filtered backprojection (RFBP), we link RFBP with the objects of the scene, and we identify the components of RFBP.

So we first define a notion of reflective projection, which is inspired from the application that is mentionned above. Some *intensity* is projected from opaque objects to a screen, along parallel rays, and for several angles of view. The emission intensity can vary with the angle; and the angles do not necessary scan a full circle. Then, with some regularity assumptions that we formulate, it is possible to define and to analyse standard tomographic filtering [9] on reflective projections, due to the distribution theory [7]. Filtered projections are written in function of the variations of the intensity: its tangential derivative on the objects, and its jumps. The next step is defining and applying the filtered backprojection, which applies the adjoint of the Radon transform on the filtered projections. We get a decomposition of the filtered backprojection in which we show how the points of the original objects contribute. We also investigate the case of a convex object as a corollary: the contribution of the shapes is distinguished from the contribution of the tangential variations of intensity.

2. Reflective projection

We consider that an object is a piecewise $\mathscr{C}^1$ simple closed curve Σ in the plane. A piecewise $\mathscr{C}^1$ function $f : \Sigma \to \mathbb{R}$ is called an emission intensity of the object Σ. If σ is a counterclockwise parametrization of Σ, then on a piece where σ and $f \circ \sigma$ are smooth, the tangential derivative $\partial_\tau f$ of the emission intensity satisfies: $(f \circ \sigma)' = (\partial_\tau f) \circ \sigma \cdot |\sigma'|$. We now consider a set of n objects: $\Sigma_i, 1 \leqslant i \leqslant n$, such that every curve Σ_i is in the exterior domain of the other curves Σ_j, $j \neq i$: see Figure 1. Let R be such that all the curves are inside the open disk $|x| < R$. Then, we consider an object Σ_0 whose interior domain contains the open disk $|x| < R\sqrt{2}$; Σ_0 is the wall of the experiment. This convention for the wall allows to treat the background exactly as the objects of the scene.

Let $\theta \in \mathrm{S}^1$ be a fixed angle. Every object Σ_i, $0 \leqslant i \leqslant n$, is assumed to have an emission intensity $y \in \Sigma_i \mapsto f_i(y, \theta)$. The index i denotes the number of the object, the first variable $y \in \Sigma_i$ is the emission point, whereas the second variable θ indicates that the intensity emission may depend on the angle θ. We measure on a screen the projection of the scene along lines which are orthogonal to $\theta = (\theta_1, \theta_2)$, or parallel to $\theta^\perp = (-\theta_2, \theta_1)$. For all $s \in [-R, R]$, the scene is projected on the screen,

Date: September 22, 2015: V4.5.

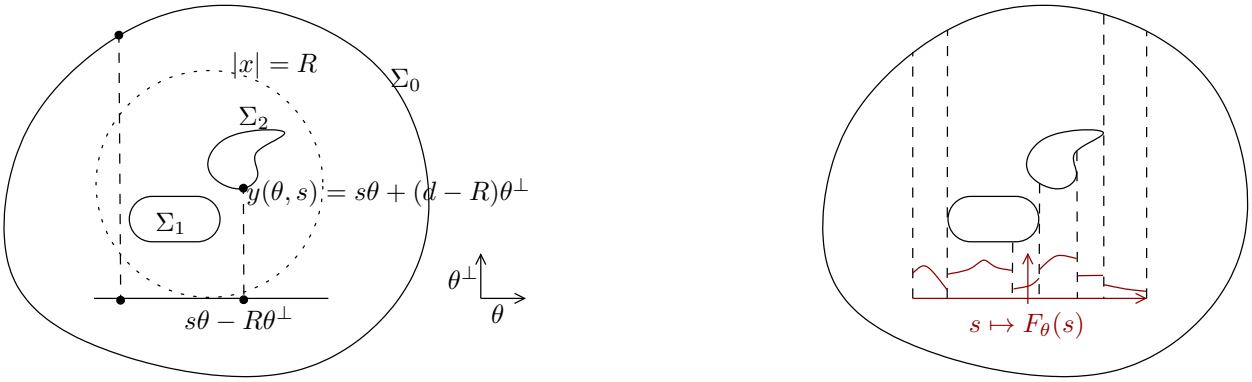

FIGURE 1. Reflective projection: the opaque objects Σ_i are projected along the direction $\theta^\perp$. On the left, the dashed lines represent two rays, from a visible point $y(\theta, s)$ to the associated screen point $s\theta - R\theta^\perp$. On the right, the piecewise smooth projection $s \mapsto F_\theta(s)$ is represented.

into the point $s\theta - R\theta^\perp$. The visible point is $y(\theta, s)$, which is the first intersection point of the line $L(\theta, s) = \{x \cdot \theta = s\}$ with the objects: $y(\theta, s) = \arg\min\{y \cdot \theta^\perp : y \cdot \theta^\perp - R > 0, y \in L(\theta, s) \cap \cup_{0 \leqslant i \leqslant n} \Sigma_i\}$. The measurement is the emission intensity of the point $y(\theta, s)$: $F_\theta(s) = f_{i(\theta,s)}(y(\theta, s), \theta)$, where $i(\theta, s) \in [0, n]$ denotes the object number of $y(\theta, s)$. The function $s \mapsto F_\theta(s)$ is a one-dimensionnal image that we call the reflective projection, associated with the angle θ. The process of reflective projection is illustrated on Figure 1; this Figure also contains an example of a one-dimensionnal image F_θ.

Notation. We denote by E the space of functions $g : [-R, R] \mapsto \mathbb{R}$ that are piecewise $\mathscr{C}^1$ and whose pieces can be extended by continuity: $g \in E$ if, and only if, there exists a (finite) subdivision $-R = s_0 < \cdots < s_j < \cdots < s_{N+1} = R$ and there exist a family of functions $g_j \in \mathscr{C}^1((s_j, s_{j+1})) \cap \mathscr{C}^0([s_j, s_{j+1}]), 0 \leqslant j \leqslant N$, such that $\forall s \notin \{s_j, j\}, g(s) = \sum_{j=0}^{N} g_j(s) \mathbb{1}_{(s_j, s_{j+1})}(s)$. For convenience we extend $g \in E$ by zero: $g(s) = 0$ for $|s| > R$.

We assume that the projection F_θ belongs to the space E, with the following piecewise smooth decomposition:

$$F_\theta(s) = \sum_{j=0}^{n_\theta} f_{i(\theta,j)}(y(\theta, s), \theta) \mathbb{1}_{(s(\theta,j), s(\theta,j+1))}(s), \tag{2.1}$$

with $-R = s(\theta, 0) < \cdots < s(\theta, j) < s(\theta, j+1) < \cdots < s(\theta, n_\theta + 1) = R$. On the piece $(s(\theta, j), s(\theta, j+1))$, the visible part of the scene is $\Sigma(\theta, j)$, subset of the object number $i(\theta, j)$: $\Sigma(\theta, j) := \{y(\theta, s), s \in (s(\theta, j), s(\theta, j+1))\} \subset \Sigma_{i(\theta,j)}$. The piece $\Sigma(\theta, j)$ is furthermore assumed to be $\mathscr{C}^1$. As in the Figure 1, the following reasons explain the apparition of jumps in the projection F_θ:

- geometrical jump: the consecutive visible pieces $\Sigma(\theta, j)$ and $\Sigma(\theta, j+1)$ are not linked: $y(\theta, s)$ jumps from one object to another object, or jumps from one part of a non-convex object to another part of the same object;
- tangential jump: the pieces $\Sigma(\theta, j)$ and $\Sigma(\theta, j+1)$ are included in the same object Σ_i and are linked, and so $y(\theta, s)$ is continuous, but the emission intensity of the object f_i jumps.

Finally, we change the acquisition angle and we restart: this experiment is repeated for θ moving in a finite set of angles $\Theta \subset \mathrm{S}^1$. Juxtaposing the different images, we get at the end a reflection sinogram $(s, \theta) \mapsto F_\theta(s)$. In the sinogram, each emission point $y \in \cup_{0 \leqslant i \leqslant n} \Sigma_i$ is seen partially (or eventually not seen) on the sinsusoid $y \cdot \theta = s$; its intensity level depends on θ.

3. Reflective tomographic filtering

Definition 3.1. A regularized kernel of the Hilbert transform is $\varphi = \mathcal{F}^{-1}(-\mathrm{i}\,\mathrm{sign}(\sigma) \cdot \hat{h}(\sigma))$, where $\mathcal{F}$ is the Fourier transform and $\hat{h}(\sigma)$ is an even windowing function with compact support (σ is the frequency).

Proposition 3.2. *Such a kernel φ is odd and belongs to $\mathscr{C}^\infty$ (with low growing derivatives).*

Definition 3.3 (Tomographic filtering)**.** Let $f \in E$ (extended by zero). Since f is in the space $\mathcal{E}'$ of distributions with compact support, it makes sense to define the tomographic φ-filtering $\partial_s f \star \varphi$ of f, and:

$$\partial_s f \star \varphi = \mathcal{F}^{-1}(|\sigma|\, \hat{h}(\sigma)\mathcal{F}(f)(\sigma)).$$

Lemma 3.4. *Let $f \in E$, with the following decomposition in E: $f(s) = \sum_{j=0}^{N} f(s)\mathbb{1}_{(s_j,s_{j+1})}(s)$. The tomographic φ-filtering of f is $\mathscr{C}^\infty$ and satisfies:*

$$\partial_s f \star \varphi(s) = \sum_{j=0}^{N} \int_{s_j}^{s_{j+1}} \partial_s f(t)\varphi(s-t)\mathrm{d}t + \sum_{j=0}^{N+1} [f]_j \varphi(s-s_j),$$

where $[f]_j := f(s_j+) - f(s_j-)$ is the jump of f accross s_j.

Proof. This result is a consequence of the jumps formula in the sense of distributions. It states that: $\partial_s f = \sum_{j=0}^{N} \partial_s f(s)\mathbb{1}_{(s_j,s_{j+1})}(s) + \sum_{j=0}^{N+1} [f]_j \delta_{s_j}$. As $\partial_s f \in \mathcal{E}'$, it can be convolved with $\varphi \in \mathscr{C}^\infty$. We get the following $\mathscr{C}^\infty$ function:

$$\partial_s f \star \varphi(s) = \langle \partial_s f(t), \varphi(s-t)\rangle = \sum_{j=0}^{N} \int_{s_j}^{s_{j+1}} \partial_s f(t)\varphi(s-t)\mathrm{d}t + \sum_{j=0}^{N+1} [f]_j \varphi(s-s_j).$$

□

Theorem 3.5 (Reflective tomographic filtering)**.** *The tomographic φ-filtering of the reflective projection $F_\theta \in E$ satisfies:*

$$\partial_s F_\theta \star \varphi(s) = \sum_{j=0}^{n_\theta} \int_{\Sigma(\theta,j)} \partial_\tau f_{i(\theta,j)}(y,\theta)\varphi(s - y\cdot\theta)\mathrm{d}\sigma(y) + \sum_{j=0}^{n_\theta+1} [f_{\theta,j}]\varphi(s - s(\theta,j)),$$

where $\partial_\tau f_{i(\theta,j)}$ is the tangential derivative of the emission intensity on the visible piece $\Sigma(\theta,j)$ and $[f_{\theta,j}]$ is an intensity jump between two pieces.

Proof. By assumption, the projection $F_\theta \in E$ has the decomposition 2.1. We apply Lemma 3.4:

$$\partial_s F_\theta = \sum_{j=0}^{n_\theta} \partial_s f_{i(\theta,j)}(y(\theta,s),\theta)\mathbb{1}_{(s(\theta,j),s(\theta,j+1))} + \sum_{j=0}^{n_\theta+1} [f_{\theta,j}]\delta_{s(\theta,j)}, \text{ with}$$

$$\begin{aligned}
\partial_s f_{i(\theta,j)}(y(\theta,s),\theta) &= \partial_\tau f_{i(\theta,j)}(y(\theta,s),\theta)\,|\partial_s y(\theta,s)|\,,\\
[f_{\theta,j}] &:= f_{i(\theta,j)}(y(\theta,s(\theta,j)+),\theta) - f_{i(\theta,j-1)}(y(\theta,s(\theta,j)-),\theta), \quad 1 \leqslant j \leqslant n_\theta,\\
[f_{\theta,0}] &:= f_{i(\theta,0)}(y(\theta,s(\theta,0)+),\theta), \quad [f_{\theta,n_\theta+1}] := -f_{i(\theta,n_\theta)}(y(\theta,s(\theta,n_\theta+1)-),\theta).
\end{aligned}$$

Thus the filtering is:

$$\begin{aligned}
\partial_s F_\theta \star \varphi(s) &= \sum_{j=0}^{n_\theta} \int_{s(\theta,j)}^{s(\theta,j+1)} \partial_\tau f_{i(\theta,j)}(y(\theta,t),\theta)\,|\partial_s y(\theta,t)|\,\varphi(s-t)\mathrm{d}t + \sum_{j=0}^{n_\theta+1} [f_{\theta,j}]\varphi(s-s(\theta,j))\\
&= \sum_{j=0}^{n_\theta} \int_{\Sigma(\theta,j)} \partial_\tau f_{i(\theta,j)}(y,\theta)\varphi(s-y\cdot\theta)\mathrm{d}\sigma(y) + \sum_{j=0}^{n_\theta+1} [f_{\theta,j}]\varphi(s-s(\theta,j)) \quad (y(\theta,t)\cdot\theta = t).
\end{aligned}$$

□

This theorem shows that a filtered image $\partial_s F_\theta \star \varphi$ contains two contributions. The first one is a φ-spreading of the tangential variations $\partial_\tau f_{i(\theta,j)}$ of the emission intensity of the visible pieces $\Sigma(\theta,j)$. The other one is a φ-spreading of the intensity jumps $[f_{\theta,j}]$ between pieces. In particular, it can be noticed that when the support of φ is small, the last contribution is a contour detection (zero-crossing) in the image F_θ.

4. Reflective filtered backprojection

The filtered backprojection is a summation over sinusoids $x \cdot \theta = s$ in the filtered sinogram:

Definition 4.1 (Filtered backprojection)**.** Let φ be a regularized Hilbert kernel and a sinogram $F : \theta \in \Theta \mapsto F_\theta \in E$. The filtered backprojection of F is:

$$x \in \mathbb{R}^2 \mapsto \mathcal{R}^*[\partial_s F_\theta \star \varphi](x) = \sum_{\theta \in \Theta} \partial_s F_\theta \star \varphi(x \cdot \theta).$$

Using the decomposition of the reflective tomographic filtering (theorem 3.5), we get the following decomposition in the reflective case:

Theorem 4.2 (Reflective filtered backprojection)**.** *If $F : \theta \in \Theta \mapsto F_\theta$ is the reflective sinogram 2.1, then its filtered backprojection with the kernel φ is:*

$$\mathcal{R}^*[\partial_s F_\theta \star \varphi](x) = \sum_{\theta \in \Theta} \left[\sum_{j=0}^{n_\theta} \int_{\Sigma(\theta,j)} \partial_\tau f_{i(\theta,j)}(y,\theta) \varphi((x-y)\cdot\theta) \mathrm{d}\sigma(y) + \sum_{j=0}^{n_\theta+1} [f_{\theta,j}] \varphi(x \cdot \theta - s(\theta,j)) \right].$$

This theorem shows that the reflective filtered backprojection (RFBP) contains two contributions. The first one is due to the tangential variations of the visible emission intensity, and the second one is due to the jumps. Furthermore the RFBP is a superposition of terms $x \mapsto A(y,\theta)\varphi((x-y)\cdot\theta)$, with $(\theta, y) \in \Theta \times \cup_i \Sigma_i$. At a *generical* point x, the contributions from different (θ, y) are generically incoherent and may compensate for each other. But coherence can appear for specific choices of x; more particularly, when the receptor x is close to a *source* y, the different (y, θ) can produce terms that are constructively added. This suggests that the highest (absolute) values of the RFBP must be located near the objects, and more particularly near points at the origin of variations or jumps in the reflective projections.

Corollary 4.3 (Convex lambertian object)**.** *We consider a scene with a unique convex object Σ. We assume that its intensity $f : y \in \Sigma \mapsto f(y)$ does not depend on θ (lambertian object). We assume that the wall Σ_0 does not emit: $f_0 = 0$. For each angle of projection $\theta \in \Theta$, the reflective projection F_θ can be decomposed in E under the form:*

$$F_\theta(s) = \sum_{j=1}^{n_\theta - 1} f(y(\theta,s)) \mathbb{1}_{(s(\theta,j), s(\theta,j+1))}(s),$$

with $\Sigma_+(\theta) = \{y \in \Sigma : \tau_y \cdot \theta > 0\} = \{y(\theta,s), s_1 < s < s_{n_\theta}\} = (\underline{y}_\theta, \overline{y}_\theta)$ being the visible part of Σ under the angle θ, and $\underline{y}_\theta, \overline{y}_\theta \in \Sigma$ being the boundary points of $\Sigma_+(\theta)$. We also introduce the finite set of boundary points where f jumps: $y_\alpha, \alpha \in A$, and the jumps: $[f_\alpha]$. The decomposition of the RFBP yields: $\mathcal{R}^*[\partial_s F_\theta \star \varphi](x) = T_{\mathrm{der}} + T_{\mathrm{jump}} + S_{\mathrm{left}} + S_{\mathrm{right}}$, with:

$$T_{\mathrm{der}} = \int_\Sigma \partial_\tau f(y) \sum_{\theta \in \Theta : \theta \cdot \tau > 0} \varphi((x-y)\cdot\theta) \mathrm{d}\sigma(y); \quad T_{\mathrm{jump}} = \sum_{\alpha \in A} [f_\alpha] \sum_{\substack{\theta \in \Theta : \theta \cdot \tau_{y_\alpha} > 0, \\ s(\theta,1) < y_\alpha \cdot \theta < s(\theta, n_\theta)}} \varphi((x - y_\alpha)\cdot\theta);$$

$$S_{\mathrm{left}} = \sum_{\theta \in \Theta} f(\underline{y}_\theta) \varphi((x - \underline{y}_\theta)\cdot\theta); \qquad S_{\mathrm{right}} = \sum_{\theta \in \Theta} -f(\overline{y}_\theta) \varphi((x - \overline{y}_\theta)\cdot\theta).$$

The term T_{der} looks like a convolution of the tangential derivative of the intensity f with a partial backprojection of the filter φ; for each *source* $y \in \Sigma$, only the angles θ such that y is visible under θ are kept in the backprojection. The term T_{jump} is very similar but is about the tangential jumps $[f_\alpha]$ at the points $y_\alpha \in \Sigma$. The term S_{left}, resp. S_{right}, comes from the jumps at the left, resp. right, boundaries $s(\theta, 1)$, resp. $s(\theta, n_\theta)$, of the object in the images F_θ. As a result, the RFBP has two contributions: $S_{\mathrm{left}} + S_{\mathrm{right}}$ which is mainly due to the shapes of Σ, and $T_{\mathrm{der}} + T_{\mathrm{jump}}$ which is due to the tangential variations (and jumps) of the intensity f.

Remark. If we assume that Θ is symmetric with respect to 0, and that the left and the right boundaries are exchanged for opposite angles: for all $\theta \in \Theta$, $-\theta \in \Theta$, and $\overline{y}_\theta = \underline{y}_{-\theta}$, then $S_{\mathrm{right}} = \sum_{\theta \in \Theta} f(\underline{y}_{-\theta}) \varphi((x - \underline{y}_{-\theta)}) \cdot -\theta)$ (φ is odd), and thus $S_{\mathrm{right}} = S_{\mathrm{left}}$ by the change of variable $\theta := -\theta$. ∎

5. Conclusion

Being applied on reflective data, the filtered backprojection has two main contributions; they are due to the jumps formula which is applied during the filtering step. One of them is explained by the jumps in the images, due to interfaces or discontinuties of the emitted intensity; the other one comes from the tangential derivative of the emitted intensity. High values are produced near the objects of the scene, and more particularly near portions of objects which generate contrasts in the projections. Such a method recalls the methods which are based on analysis of sensitivity/variations (gradient, topological derivative,...): an operator which concerns variations is applied (filtered backprojection here), the regions of interest are located near the highest values of the result.

A classical extension of the 2D filtered backprojection is the FDK algorithm, which is dedicated to transmission projections, in the 3D cone-beam scanning geometry. In a word, perspective projections of the scene are considered; the center of projection scans a horizontal circle around the scene. The two main steps of the FDK algorithm are the same than the 2D filtered backprojection: the first one is a 1D-filtering with a regularized Hilbert kernel, in the horizontal direction; the second one is a backprojection along the rays of projection. So the results about the RFBP can be extended to the FDK algorithm. This gives a meaning and a new light on the FDK algorithm when it is applied on reflective projections. This shows that the reflective FDK reconstruction is essentially produced by the horizontal variations (and the horizontal jumps) in the recorded images. In particular, the features of the scene that are transverse to horizontal planes are emphasized: they tend to produce horizontal contrasts.

References

[1] J.-B. Bellet, I. Berechet, S. Berechet, G. Berginc, and G. Rigaud. Laser Interactive 3D Computer Graphics. *2nd International Conference on Tomography of Materials and Structures, Québec*, 2015. <hal-01175855>.

[2] G. Berginc. Scattering models for range profiling and 2D-3D laser imagery. In L. M. Hanssen, editor, *Reflection, Scattering, and Diffraction from Surfaces IV, 92050K*, volume 9205 of *Proc. of SPIE*, 2014.

[3] G. Berginc and M. Jouffroy. Optronic system and method dedicated to identification for formulating three-dimensional images. US patent 20110254924 A1, European patent 2333481 A1, FR 09 05720 B1, November 2009.

[4] G. Berginc and M. Jouffroy. Simulation of 3D laser systems. In *Geoscience and Remote Sensing Symposium, 2009 IEEE International, IGARSS 2009*, volume 2, pages 440–444. IEEE, 2009.

[5] G. Berginc and M. Jouffroy. Simulation of 3D laser imaging. *PIERS Online*, 6(5):415–419, 2010.

[6] G. Berginc and M. Jouffroy. 3D laser imaging. *PIERS Online*, 7(5):411–415, 2011.

[7] J.-M. Bony. *Cours d'analyse: théorie des distributions et analyse de Fourier*. Editions Ecole Polytechnique, 2001.

[8] F. Knight, S. Kulkarni, R. Marino, and J. Parker. Tomographic Techniques Applied to Laser Radar Reflective Measurements. *Lincoln Laboratory Journal*, 2(2), 1989.

[9] F. Natterer and F. Wübbeling. *Mathematical methods in image reconstruction*. SIAM, 2007.

[10] J. Sharpe. Optical projection tomography as a new tool for studying embryo anatomy. *Journal of anatomy*, 202(2):175–181, 2003.

Universite de Lorraine, Institut Elie Cartan de Lorraine, UMR 7502, Metz, F-57045, France, CNRS, Institut Elie Cartan de Lorraine, UMR 7502, Metz, F-57045, France.
E-mail address: jean-baptiste.bellet@univ-lorraine.fr

Thales Optronique, 2, Avenue Gay Lussac CS 90502, 78995 Élancourt Cedex, France.
E-mail address: gerard.berginc@fr.thalesgroup.com